



CARE-HIPPI WP3 FINAL REPORT
Superconducting structures

Juliette Plouin¹

1) CEA-Saclay, Gif-sur-Yvette, France

with contributions of:

INFN Milano, Italy

CEA Saclay, France

Forschungszentrum Jülich, Germany

IPN Orsay, France

IAP Frankfurt, Germany

Abstract

In the frame of the CARE-HIPPI program, five laboratories were in charge of studying solutions with superconducting structures for a proton injector. The work achieved during this five years program has led to the realization of superconducting cavities, and has given meaningful results for the RF and mechanical tests. Associated elements like fundamental power couplers and tuning systems have also been realized. This report summarizes this work and presents the design of the structures with RF and mechanicals considerations, the fabrication of the cavities and the experimental measurements. Elements of comparative assessments are also given.

I. Introduction

A. CARE – HIPPI / WP3

In the frame of the High Intensity Pulsed Proton Injector (HIPPI) project, the Work Package 3 (WP3) was in charge of studying solutions with superconducting structures. The laboratories involved in this WP3 studied and developed different types of structures, and prepared for comparative assessment. It was expected to reach gradients higher than 7 MV/m with a quality factor higher than 10^{10} in the energy range 100-200 MeV, at a construction cost comparable to normal-conducting structures.

Moreover, the construction of a high power 704 MHz RF test place for RF cavities had to be achieved.

B. Outline of the report

The different cavities tested in the frame of this project are presented in section II, where their RF parameters are detailed.

This report will lead to comparative assessments of the different structures and it is more consistent to compare cavities with the same range of β . The comparison will thus be developed between cavities operating at close beta: CH structure with beta 0.15 single spoke cavity and triple spoke with elliptical cavities.

According to this choice, the report is divided in two main sections.

- Section III contains information and results about the three cavities with $\beta = 0.5$: both elliptic cavities and triple spoke at 352 MHz.
- Section IV gives the parameters and test results for the two cavities with low β : the single spoke and the CH structure; the results for the RF tests of the triple spoke at 760 MHz are also given in this section.

These sections start with calculations and results on the mechanical parameters of the structure. Indeed, as the cavities developed in the HIPPI program are aimed to work in the pulsed mode, the sensitivity to the Lorentz force is especially critical. It is thus of high importance to reduce as much as possible the effects of the Lorentz force detuning for the cavities. This requires the use of several elements in the design such as stiffening rings or ribs, to enhance the stiffness of the cavities which are detailed. All the laboratories have carried out simulations to evaluate the influence of the Lorentz Force Detuning (LFD) on their structures. Experimental results have been obtained for the LFD, which are compatible with the numerical results. Four of the laboratories (INFN, CEA, IPNO and IAP), were also involved in the realization of a tuning system for their cavity, working both in the slow and fast regime. The choices for the design of these tuners are presented in this report, together with some results.

All the cavities have been tested at low power, and the tests results are given, with Q_0 vs E_{acc} curves. As the performances of the cavities strongly depend on their surface preparation, all the steps of the preparation are detailed and the procedures of tests are described. Moreover, to allow consistent comparison, it was necessary to be coherent for the choice of several parameters. For example, the same definition for E_{acc} has been

chosen for all the cavities: $E_{acc} = V_{acc}/L_{acc}$, where V_{acc} is the accelerating voltage and L_{acc} is the accelerating length given by $L_{acc} = N_{gap} \cdot \beta \cdot \lambda / 2$.

CEA and IPNO were also in charge of the design and fabrication of a High Power Couplers for respectively elliptical and spoke cavities. In parallel, a high power 704 MHz RF test place has also been built at CEA and is ready for RF tests.

In section V, conclusions and perspectives are given about the work achieved in the frame of HIPPI/WP3. Considerations about the real estate gradient are discussed, and some conclusions about the elements of comparison emerging from the report are given.

II. Presentation of the cavities - RF parameters



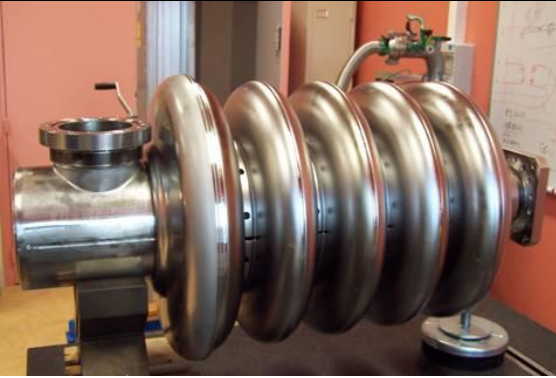



A. The cavities

The types and main parameters of the cavities developed and fabricated in WP3 are detailed in the table below. The other critical elements (such as tuners and couplers) developed in the frame of the program are also indicated. One has to notice that some cavities already existed before the beginning of the program.

Lab.	Type	In the frame of HIPPI	β -design	Gaps	Freq. (MHz)
INFN	Elliptical	Tuning system + He tank + RF tests	0.47	5	704
CEA	Elliptical	Cavity + Tuning system + He tank + coupler + RF tests	0.47	5	704
FZJ	3 Spoke	Cavity + coupler (IPN)	0.48	4	352
FZJ	3 Spoke	Tests	0.2	4	760
IPNO	1 Spoke	Cavity + coupler + He tank + Tuning system	0.15	2	352
IAP	CH	Tuning system	0.1	19	352

Table 1 : the HIPPI WP3 program

All the cavities have been fabricated at the end of the program, as shown on the following photos. Design parameters, fabrication steps of the different elements and experimental results will be detailed in the report. For the 3-Spoke at 760 MHz, only the RF tests were in the frame of the program, and their results are given in section IV.C.1

<p>Elliptic A / INFN / $\beta = 0.47$</p>  <p>A photograph of a cylindrical metal component with a series of six elliptical vanes arranged along its length. It has two flange-like ends.</p>	<p>3 Spoke / FZJ / $\beta = 0.48$</p>  <p>A photograph of a vertical cylindrical metal structure with three spokes extending from the center to the outer shell. It is mounted on a stand with wheels.</p>
 <p>A photograph of a cylindrical metal component with a series of six elliptical vanes, similar to the Elliptic A design, but with a different internal structure.</p>	<p>3 Spoke / FZJ / $\beta = 0.2$</p>  <p>A photograph of a compact, rectangular metal component with three spokes extending from the center to the outer shell. It has several ports and a valve.</p>
 <p>A photograph of a spherical metal component with a single spoke extending from the center to the outer shell. It has several ports and a valve.</p>	 <p>A photograph of a spherical metal component with three spokes extending from the center to the outer shell. It has several ports and a valve.</p>

B. RF parameters

The design guidelines for each cavity of the HIPPI project have led to an optimisation of each geometry, resulting in a set of RF parameters. The number of gaps and the kind of superconducting structure result of a choice of prototype operating at the given frequency with the given beta. The following table shows the RF parameters calculated for each cavity.

	Elliptic A INFN	Elliptic B CEA	Triple Spoke FZJ	Single Spoke IPN	CH IAP - FU
Number of gaps (N _{gap})	5	5	4	2	19
Frequency [MHz]	704	704	352	352	352
Geometrical Beta	0.47	0.47	0.48	0.15	0.1
B _{pk} /E _{acc} [mT/(MV/m)]	5.88	5.59	10.97	14.48	7.28
E _{pk} /E _{acc}	3.57	3.36	4.65	6.74	6.56
G [Ohm]	160	161	101	67	56
Cell to cell coupling	1.34 %	1.35 %	N/A	N/A	N/A
r/Q [Ohms]	180	173	420	108	3220
Beam diameter aperture [mm]	80	80	50	56	28
L _{acc} = N _{gap} .β.λ/2 [mm]	500	500	818	170	810
Operating Temperature (O.T.)	2 K	2 K	4.2 K	4.2 K	4.2 K
R _{BCS} @ O.T. (theoretical)	3.2 nΩ	3.2 nΩ	39 nΩ	39 nΩ	39 nΩ
Q ₀ @ O.T. for R _{BCS}	5.10 ¹⁰	5.10 ¹⁰	2.6*10 ⁹	1.7*10 ⁹	1.4*10 ⁹

Table 2 : RF parameters

The values for the BCS resistance given in this table have been calculated for all the cavities with the same formula: $R_{BCS} = 2.10^4(1/T).(f/1.5)^2.exp(-17.67/T)$, where f is the frequency in GHz and T the operating temperature. R_{BCS} is thus much lower for 2K than for 4.2K.

The value B_{pk}/E_{acc} is an important parameter to estimate the maximum accelerating field expected in a structure, and has to be as low as possible.

III. Cavities β = 0.5

A. General information about the prototypes – mechanicals

1. Miscellaneous

	Elliptic A INFN	Elliptic B CEA	Triple Spoke FZJ
Nominal wall thickness [mm]	4	4	4
Length of the cavity (mm) (bridle to bridle)	870	832	780
Flanges material	NbTi	St. Steel	St. Steel

Helium tank material	Ti	St. Steel	N/A
Magnetic shield	Yes	Yes	Supplied by cryostat

Table 3 : miscellaneous parameters

A specific magnetic shield has been fabricated for both elliptic cavities, while the shielding is supplied by cryostat for the other cavities. The magnetic shield is placed inside the helium tank for elliptic A (Figure 1), and outside the helium tank for elliptic B (Figure 2).

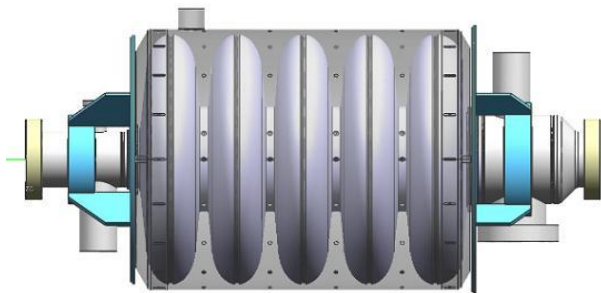


Figure 1 : Internal magnetic shield for elliptic A

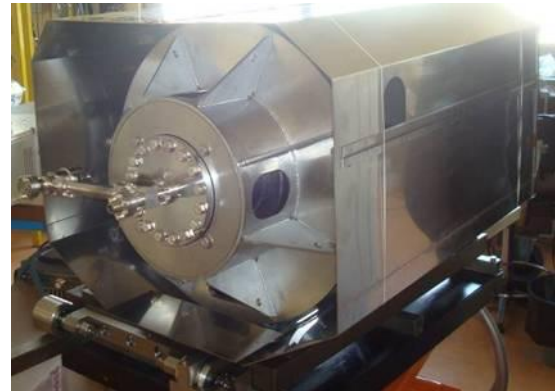


Figure 2 : External magnetic shield for elliptic B

2. Stiffening systems

Elliptic A

One five cell SC cavity was developed at INFN Milano and built in 2002. The cavity is provided with a set of stiffening between the cells in order to lowering the effects of the Lorentz Forces (see Figure 3).

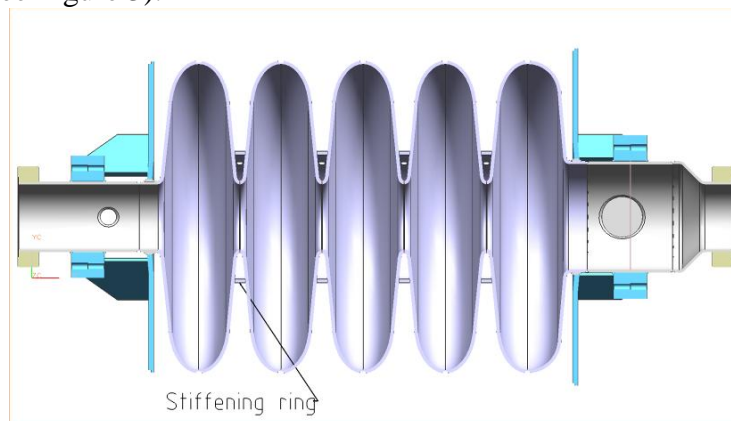


Figure 3 : cavity A section with stiffening rings

Because the LFD strongly depends on the external stiffness seen by the cavity (see Figure 4), one of the main requirements that the helium tank and tuning system must satisfy is to have a sufficiently high axial stiffness. With a design accelerating field of 8.5 MV/m, the overall K_L in the operating condition should be limited below $-10 \text{ Hz}/(\text{MV/m})^2$ to allow for LFD compensation by the LLRF system. In order to achieve this condition the combined stiffness of the He Tank and tuning system needs to be greater than 9 kN/mm.

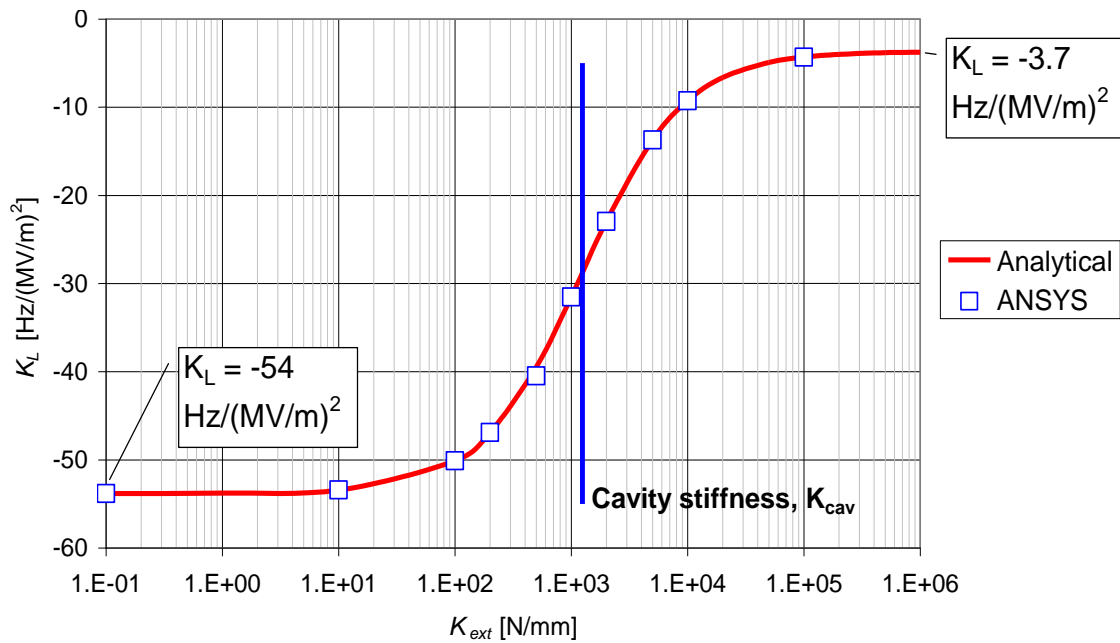


Figure 4: Lorentz force detuning coefficient as a function of external stiffness

Elliptic B

The cavity thickness is fixed to 4 mm, except in the equator weld region where a reduction to 2 mm was taken into account in the calculations. A high power coaxial fundamental power coupler is developed in the project, which has 100 mm in diameter. The impact of such coupler characteristics combined with external Qs in the range $5 \cdot 10^5$ to 10^6 , is a large beam tube diameter, in our case 130 mm. The beam tube which supports the FPC is enclosed in the stainless steel helium vessel for two reasons. First the coupler is very close to the iris of the adjacent cell, which has to be mechanically stiffened, the connection of the helium vessel to the beam tube would have required more space. Second, it is easier to stiffen the helium tank itself with four welded wings



Figure 5 : elliptic A cavity without helium tank

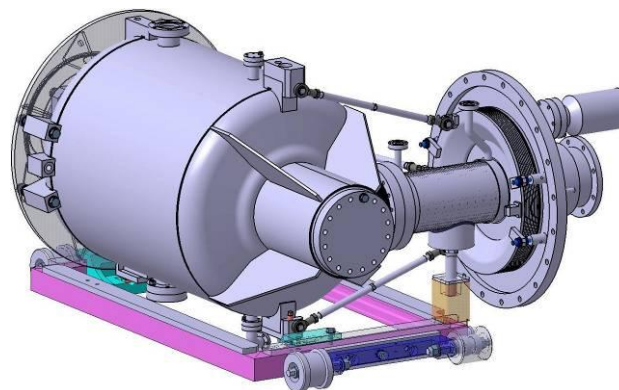


Figure 6 : complete cavity equipped with the helium vessel and vacuum part of the FPC.

A first optimization of one set of rings gave an optimal position at $R1 = 62$ mm. A second set of rings added at a greater radius $R2 = 110$ mm can help reducing the sensitivity of the static Lorentz coefficient to the cavity boundary conditions. Extra stiffeners are also located around

the end cells irises on the beam tube side. This is mandatory to get a balanced stiffness across all the cells.

The cavity profile with all the stiffening system is shown on Figure 7. The variation of the Lorentz detuning with the external stiffness of the system is shown on Figure 8, showing the role of the second set of rings, especially for very low values of K_{ext} (free ends).

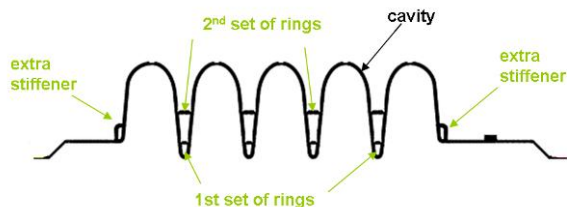


Figure 7 : stiffening system of elliptical B

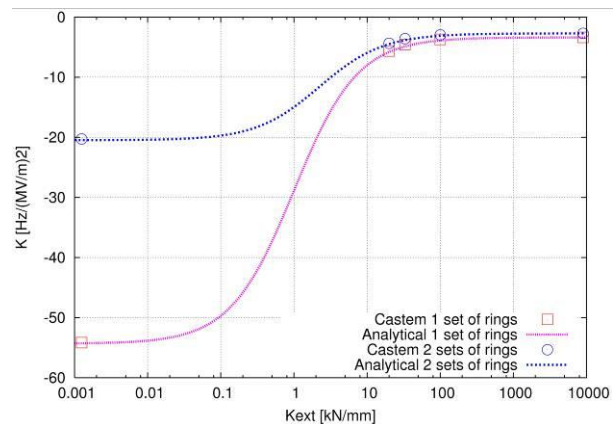


Figure 8 : Lorentz detuning (KL) vs external stiffness (K_{ext}) with 1 or 2 sets of rings

Triple Spoke

The whole of our RF design has been greatly adapted to two main goals - the simplest technology of cavity manufacture and for the prime goal of the project to achieve the best possible structural parameters (Lorentz force frequency shift and frequency pressure dependence). In our case, racetrack/elliptical spoke base shapes have been also under consideration but found to be more complicate for manufacture and the circular conical shape have been accepted. Also, the cavity square cross section is much less rigid rather cylindrical and requires very complicate stiffening structure. The final geometry of the cavity is shown in Figure 9.

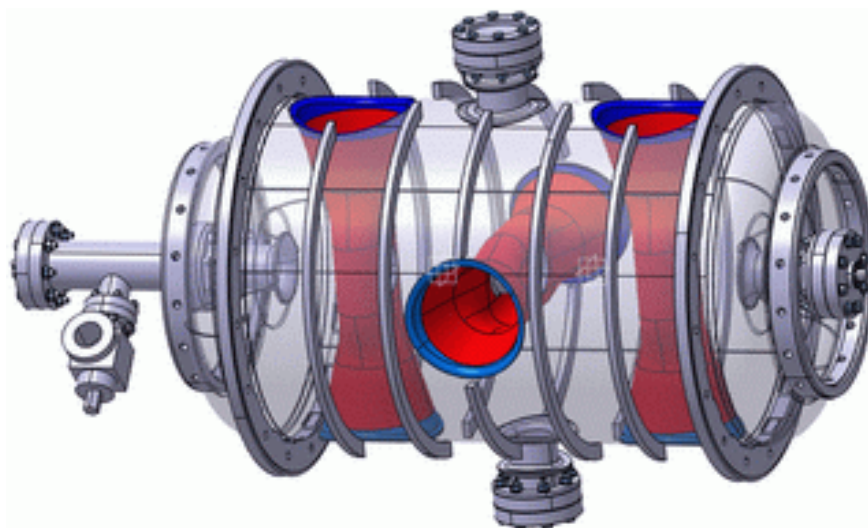


Figure 9 : 352 MHz Triple-Spoke superconducting prototype

The strategy of cavity structural design should include the integrated simulations of RF and mechanical properties. The uncertainty with the cavity final wall thickness changes the results of the structure optimisations and should be taken into account. The final thickness of 4 mm of cavity walls for calculations is supposed. The stiffening structure of the prototype consists

of five series of niobium ribs (10mm x 20mm) welded on cylindrical cavity body, two rings (18mm x 40mm) welded at the extremities of the cylinder and a niobium ring (18mm x 35mm) at each end cup (Figure 9). Neither helium vessel nor tuner is equipped on this prototype, no rigid fixation is supposed and as consequences, the boundary conditions correspond to externally unconstrained cavity.

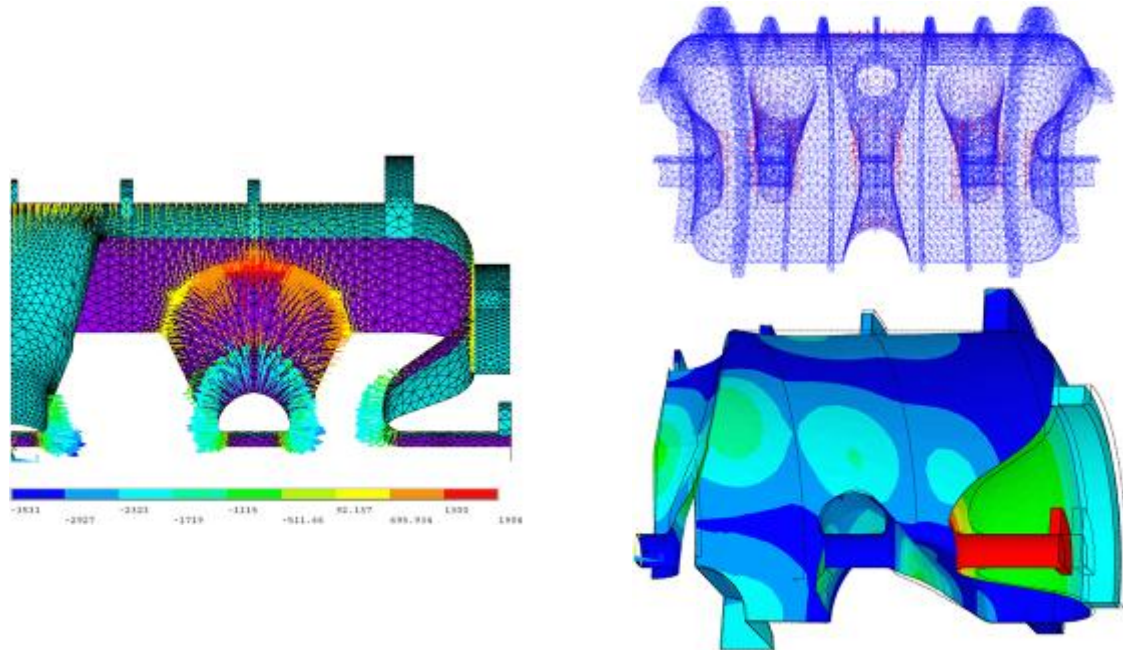


Figure 10 : Lorentz force distribution on the cavity's wall and cavity deformations caused by Lorentz forces.

The cavity structural behaviour can be accurately generalized to the case of arbitrary boundary conditions, characterized by its longitudinal stiffness K_{ext} , (Figure 11) because of the environmental cryomodule structure.

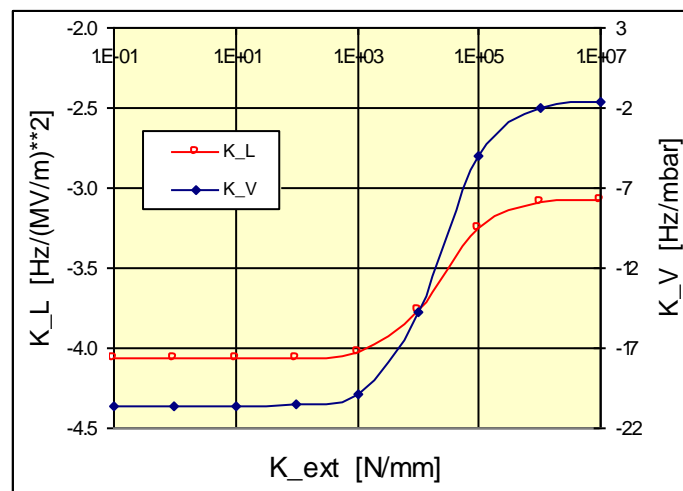


Figure 11: Cavity structural analyses results.

3. Mechanical parameters / comparison

The mechanical parameters calculated for the prototypes are presented in this section for the 3 cavities with $\beta = 0.5$. Several parameters are given in Table 4. The influence of the Lorentz

Force Detuning (LFD), which is a critical point for these cavities which are aimed to work in a pulsed mode, is given by the Lorentz coefficient K_L in $\text{Hz}/(\text{MV}/\text{m})^2$. K_L depends strongly on the external stiffness, which is not easy to evaluate in the test conditions. Meaningful information must also contain the extreme values of K_L (free ends/fixed ends), and the theoretic curve between these points, which is shown in Figure 12.

	Elliptic A INFN	Elliptic B CEA	Triple Spoke FZJ
Cavity stiffness K [kN/mm]	1.25	2.25	22.4
Tuning sensitivity $\Delta F/\Delta l$ [kHz/mm]	353.4	295	182.7
Pressure sensitivity [Hz/mbar] (fixed ends)	84.7	29.2	21.4
K_L with fixed ends [$\text{Hz}/(\text{MV}/\text{m})^2$]	-3.7	-2.7	-3.1
K_L with free ends [$\text{Hz}/(\text{MV}/\text{m})^2$]	-54	-20.3	-4.1
K_L measured during cold tests (detailed in section C.2) [$\text{Hz}/(\text{MV}/\text{m})^2$]	[-47 ; -20]	-3.8 ± 0.4	-5.5

Table 4 : mechanical parameters

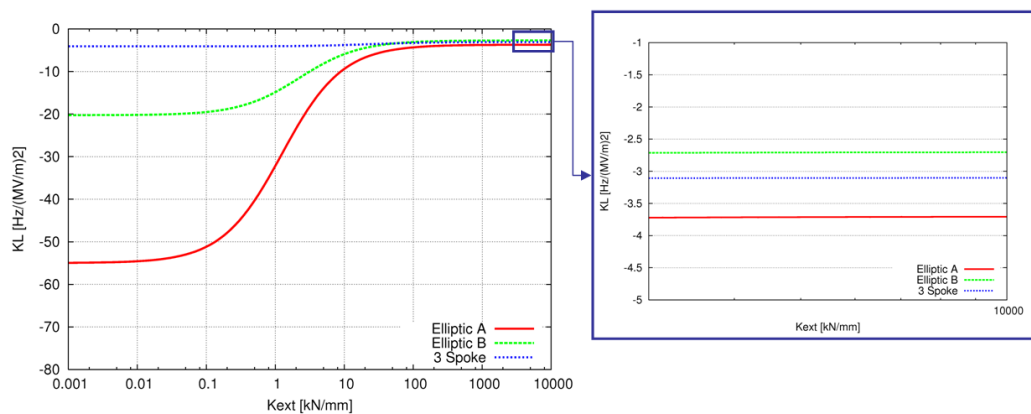


Figure 12 : Lorentz detuning (K_L) vs external stiffness (K_{ext}). Spot @ high K_{ext} (~ fixed ends)

It appears that the cavity stiffness is much higher for the triple spoke cavity ; the difference between elliptic A and elliptic B for the stiffness is mainly due to the second set of stiffening rings which have been placed between the cells of elliptic B.

Concerning the LFD, values for K_L @ fixed ends shown on the spot of Figure 12 give the minimum Lorentz detuning expected for each cavity. The smallest $|K_L$ @ fixed ends| is obtained for elliptic B. When the difference $|\Delta K_L(\text{free ends}/\text{fixed ends})|$ is small, like for the triple spoke, the external stiffness is not a critical value to have a small Lorentz detuning. If difference $|\Delta K_L(\text{free ends}/\text{fixed ends})|$ is high, then the external stiffness has to be high enough (~ 100 kN/mm). For the elliptic B, the stiffness of the tuner (which gives the external stiffness during the tests) should be of this order of magnitude.

The values for the measured K_L , obtained during cold tests, show that the experimental data are compatible with the simulations. However it is difficult to evaluate the external stiffness during the tests. More information is given about these mechanical measurements in section C.2.

4. Tuning systems

The tuning system had to be designed and fabricated for both elliptic cavities.

Elliptic A

The tuner has been fabricated. It is a blade tuner, placed between two parts of the helium tank

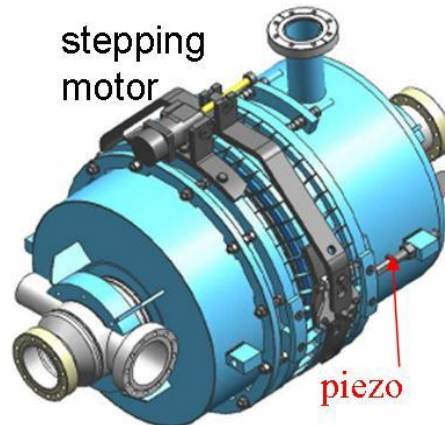


Figure 13 : blade tuner for elliptic B

The expected values for the tuning system are given as follow:

Slow tuning: Tuning Range = ~ 420 kHz

- Tuner excursion is 1.3 mm, with present leverage
- Spring analysis: 93% of tuner excursion transferred to cavity
- Frequency sensitivity is 350 kHz/mm

Fast tuning: LFD Compensation = ~ 920 Hz

- We assume a 3 μm stroke to cavity, at cold (long piezos) comforted by SRF/WP8 activities
- Spring analysis: 87.6% of piezo excursion transferred to cavity

Elliptic B

We have developed a fast piezo tuner based on the Saclay-II tuner design [4] built and tested on a 1.3 GHz 9-cell Tesla type cavity. The main difference is the size of the system, and the piezo support which consists of a stainless steel elastic frame holding a single 30 mm piezo stack. It is designed in order to apply an adjustable preload on the piezo, limiting the influence of the spring constant of the cavity. The slow tuning range is ± 2.5 MHz. The tuner is attached between the He tank and the square shaped beam tube flange opposed to the power coupler port. Care has been taken in order the tuner not increase the overall length of the cavity (Figure 14).

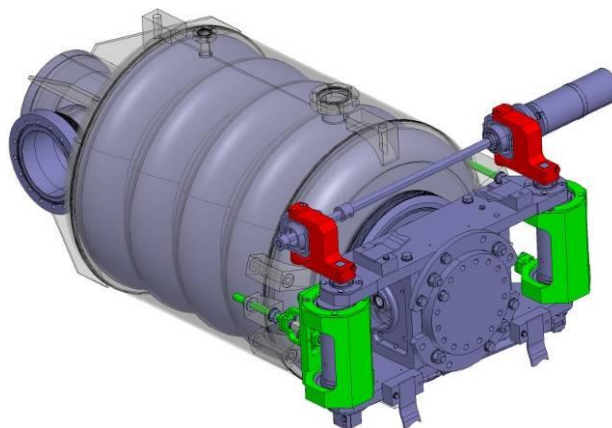


Figure 14 : Elliptic B cavity equipped with He tank and piezo tuner

B. Controls and tuning of the cavity

After the fabrication of the cavity, several controls have to be done to compare the characteristics of the cavity with those of the model. Geometrical parameters such as the length or the thickness of the cavity are measured. RF controls at room temperature are realized: operating frequency, field flatness. Then the cavity may be tuned to come close to the desired RF characteristics.

Elliptic B

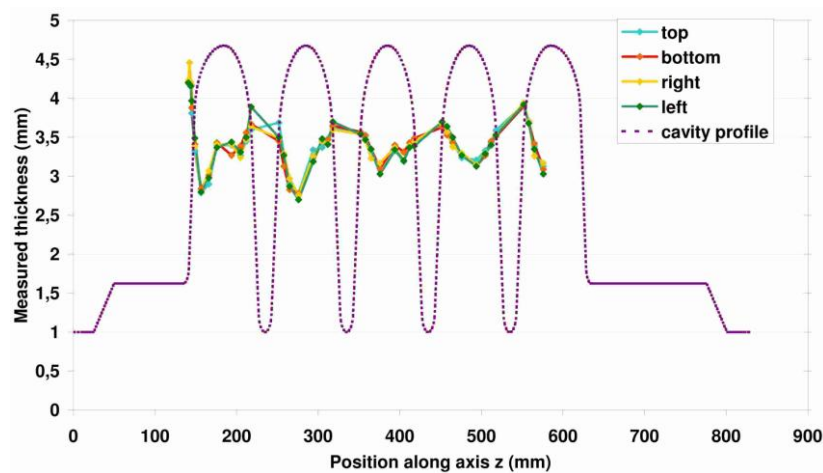


Figure 15 : thickness measured at four radial positions of the cavity

The thickness of the walls has been measured after reception of the cavity from the manufacturer, and before chemical treatments. It appeared that the effective thickness was lower than expected, about 3.3 mm instead of 4 mm (Figure 15)

The initial frequency measured after reception of the cavity was also lower than expected, with a bad field flatness, and we had to tune the cavity (whole cavity and cell per cell) to reach a frequency close to the design frequency.

C. Cold tests

1. Treatments for the cavity and RF tests

Elliptic A

Cavity A has been tested at JLAB (see Figure 16) and Saclay and it well fulfilled the requirements of the project in terms of accelerating field, with ample margins.

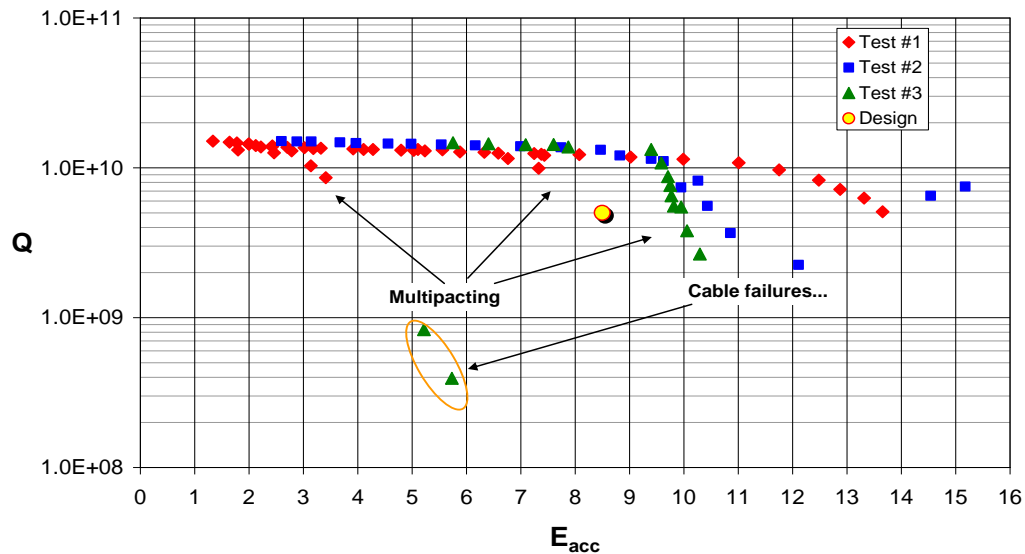


Figure 16 :Results of several vertical test on cavity Z501 performed at JLAB

Elliptic B

The cavity was heat treated to prevent Q disease (650 °C, 24 h). It had to be adjusted to recover the field distribution. The chemical treatment consisted in buffered chemical polishing (BCP) using a 1:1:2.4 FNP mixture. First a 100 µm thickness has been removed before checking the field flatness. Then 20 extra µm were removed from the surface before the high pressure rinsing (HPR) and clean room assembly. The first cavity test was plagued by field emission. It was decided to carry out the last steps of Helium tank welding. After this last fabrication step, the field flatness was checked again and it was reduced to 89 %. A new preparation was carried out, consisting of 20 µm BCP, a 2.5 h HPR in the clean room.

The cavity was measured in a vertical cryostat after a fast cool-down. The $Q_0(E_{acc})$ characteristic curve at $T = 1.8$ K is shown on figure 2. A multipactor (MP) barrier was encountered between 8 and 10 MV/m. It was processed in about 2 hours. The field emission onset field is 10 MV/m. The electron loading becomes significant (detuning observed) above 13 MV/m and could not be processed. The cavity operation was limited by a thermal quench. At the maximum $E_{acc} = 15$ MV/m, the peak surface fields are $E_{pk} = 50$ MV/m and $B_{pk} = 83$ mT. After this test, the cavity was vacuum baked using standard parameters (115 °C for 70 h) inside the vertical cryostat and cooled down again without any venting or processing. The BCS surface resistance was reduced by 25%. The MP barrier reappeared, and the processing took 3 hours, longer than before baking, which might be explained by an increase in the SEE coefficient. However, the cavity performance at 1.8 K was not changed by the baking process.

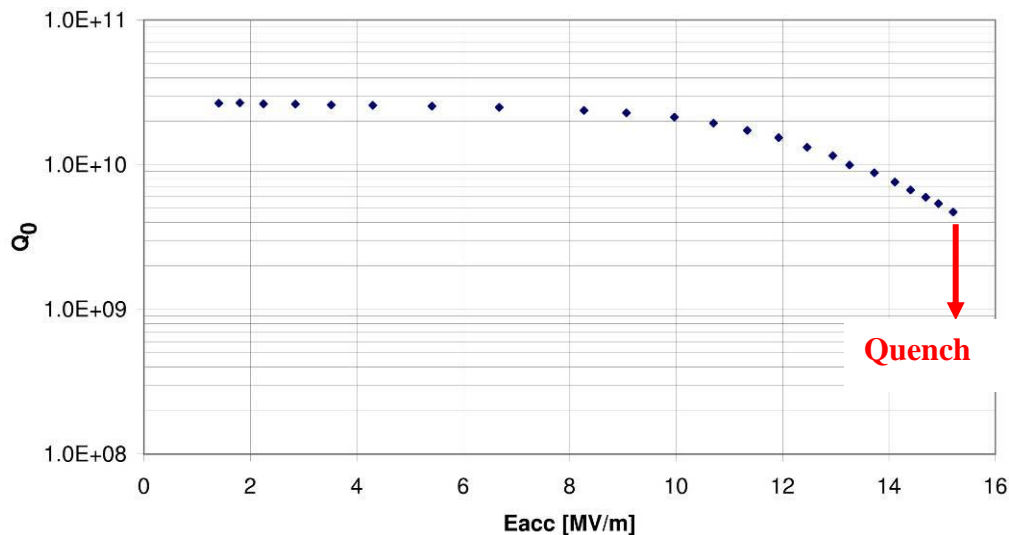


Figure 17 : RF tests results : Q_0 vs E_{acc} curve for elliptic B

Triple Spoke

The triple-spoke cavity received its chemical treatment (BCP) at Saclay. Two BCP runs were made, each with the cavity in horizontal position, sending the acid in via the lower coupler port, and taking the out coming fluid from all three other openings back to the closed acid circulation system (Fig.4). Filling and emptying took about 8 minutes. Fresh acid circulated for about 70 minutes through the cavity. For the second run the flanges were detached, and the cavity was turned about the horizontal axis by 180 degrees before the flanges were re-attached again. Totally approximately 100 μm of Niobium were removed. Still, the ultra sonic measurements indicated that the removal was not homogeneous reaching in some places only 60 μm .

The cavity was subsequently high pressure rinsed at IPN-Orsay. The standard nozzle designed for elliptical cavity was used. All four ports were used for rinsing; the rinsing was done in 4 positions, every time the rinsing water was pumped from the bottom. After the HPR the cavity was dried in a class 10 clean room for several hours and then all auxiliary parts such as blank flanges, input and output probe and pump out port with valve were assembled.

Preparation of the cavity for insertion into the vertical bath cryostat included attaching thermo-elements, installing a siphon for removal of He gas from the lower end cap, installing RF lines for (critical) coupling and for the field probe, line for vacuum pump, etc (Fig.5). Cool-down revealed no problems. The first measurements have been provided by 4K. At $E_{acc}=5.8$ MV/m the test has been stopped by the cavity quench. There was a MP discharge at around $E_{acc}=1$ MV/m, but it was processed without problems. For the second measurement the upgrade of our testing facility for 2K operations has been made. The test has been stopped by a strong MP discharge at about $E_{acc}=5$ MV/m. Fig.6 shows the Q vs E_{acc} performance of the cavity in both tests at 4.2K and at 2K.

The sensitivity of the cavity frequency to the pressure in the helium bath is measured $df/dp_{exp}=-31.9$ Hz/mbar with estimated $df/dp_{calc}=-21.4$ Hz/mbar. The Lorentz force detuning during the high power test at 4.2 and 2K was measured showing the same results $K_{L_{exp}}=-5.5$ Hz/(MV/m)² with $K_{L_{calc}}=-4.1$ Hz/(MV/m)².



Figure 18 : Triple-spoke cavity at FZJ test stand.

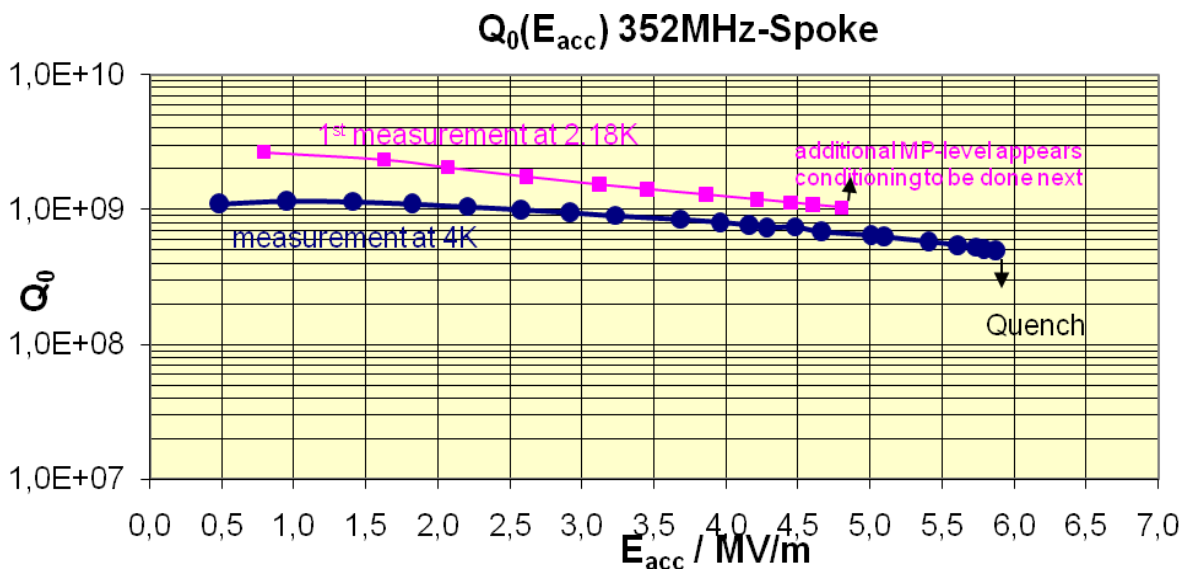


Figure 19 : RF tests results : Q_0 vs E_{acc} curve for triple spoke

2. Mechanical measurements

Elliptic A

During the cold tests the Lorentz force detuning (LFD) coefficient was also derived: the values obtained were larger than expected and with a relevant spread (Figure 20), but this is

mainly due to the uncertainty of the external constraints applied to the cavities during the tests.

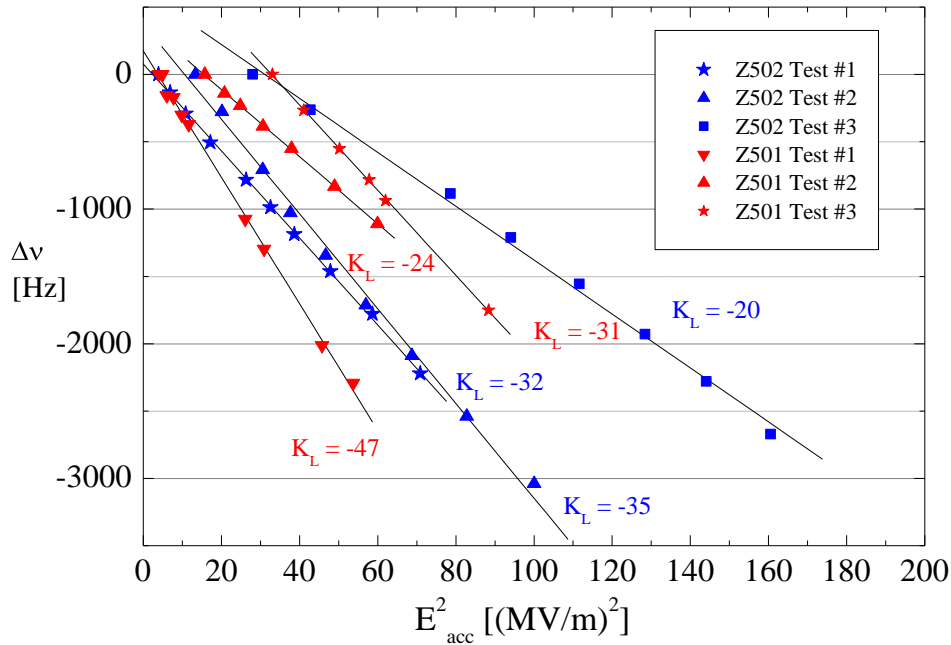


Figure 20: LFD coefficient from the test performed at JLAB (Z501) and Saclay (Z502)

Elliptic B

In order to keep the cavity length as constant as possible, a stiffening tube linking the helium tank to the otherwise free cavity end was installed at the position of the tuning system (see fig.1). This spacer ensures a high external stiffness K_{ext} to allow the static K_L to be measured in optimal conditions. Its efficiency can first be assessed when pumping on the He bath to reach 1.5 K. The He pressure drops from atmospheric pressure to a few mbar. The cavity detuning is recorded during this phase (Figure 21). The pressure sensitivity df/dP is -14.5 Hz/mbar and is very sensitive to K_{ext} . The measurement of the static K_L at 1.8 K is shown on Figure 22. Due to slight temperature variations during the measurements, the He pressure was not constant; therefore the data have been corrected using the experimental df/dP coefficient. The data set is limited to $E_{acc} < 13$ MV/m since above this value, the cavity is loaded with field emission electrons. The field measurement accuracy is estimated to 5% so K_L is evaluated at -3.8 ± 0.4 Hz/(MV/m)². It is very close to the design value of with $K_{ext} = 30$ kN

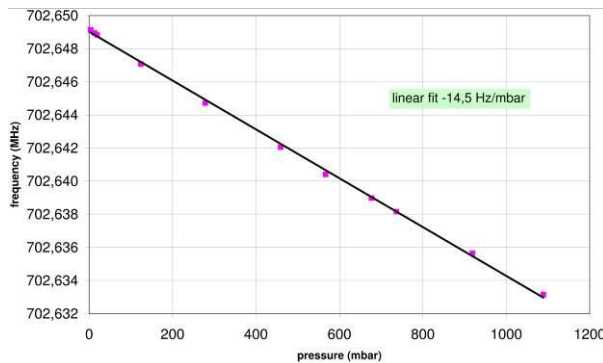


Figure 21 : Cavity frequency vs helium pressure

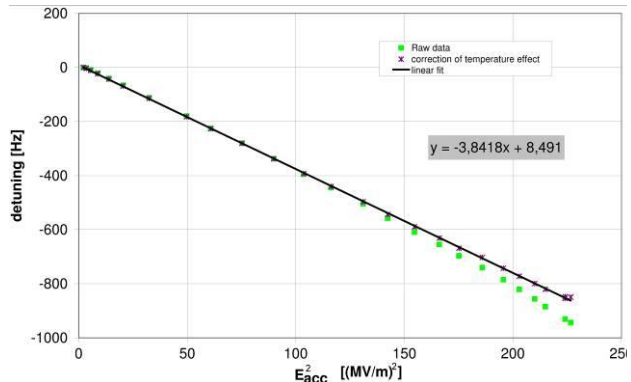


Figure 22 : Frequency detuning vs E_{acc}^2

D. RF couplers

The conception and fabrication of a RF coupler was planned for the elliptic B, and this has been achieved. Concerning elliptic A, no coupler was envisaged, and for triple spoke, the fabrication of a coupler at IPNO is prepared.

Elliptic B

The peak power requirement to operate a cavity at 12 MV/m for typical beam current of 40 mA is around 120 kW. The power needed for the higher energy part of high intensity proton linacs such as SPL rises to 1 MW. We have aimed our design at this higher power levels. The duty cycle is targeted at 10% (100 kW average power). The design is similar to the KEK-B and SNS design, build around a coaxial disk window, and 100 mm coaxial line. The air part consists of a doorknob, which connects to a WR1150 waveguide (Figure 23).

The RF window is adapted from the KEK-B window, build around a ceramic disk. The RF adaptation is obtained using chokes on both inner and outer conductors. The coupler antenna is made of electropolished OFE copper to minimize thermal radiation on the Nb coupler port and beam tube. It is electron beam welded to the window. Water cooling channels for the antenna are passing through the window core. The return channel is connected to the inner cooling channel of the ceramic. These coaxial cooling channels are connected to those of the inner conductor on the air-side, the inlet and outlets being at the doorknob. The cold part of the coupler is a 100 mm in diameter, 50 Ω coaxial line. The outer conductor is a double walled stainless steel tube enclosing three separate spiral cooling channels. A counter-flow of He gas is used to adjust the temperature distribution along the conductor when operated in the cryomodule. The outer conductor has been plated with 10 microns copper at CERN, using microwave sputtering (Figure 23). The base of the coupler port on the cavity is contained in the He tank.

The length of the air side coaxial line is mostly constrained by the position of the cavity inside CryHoLab and the diameter of the vacuum vessel. The doorknob is made of aluminium. The knob itself is CNC machined to achieve mechanical tolerances. The junction between the antenna and the knob is of sliding type, so it can be electrically insulated to bias the inner conductor if needed during the conditioning. As expected, their bandwidth is only a few MHz.

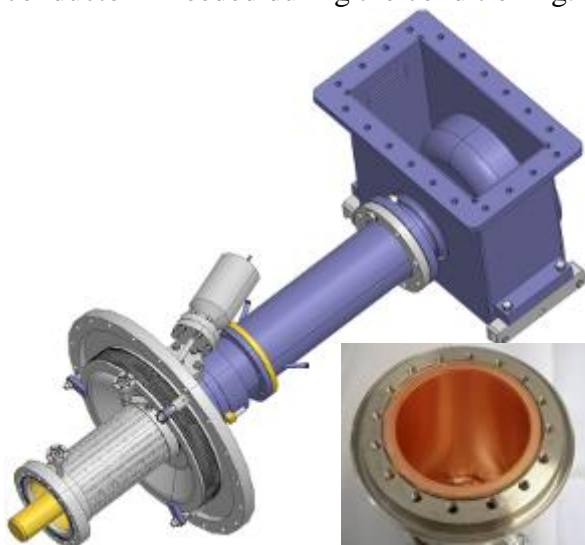


Figure 23 : Overall view of the 704 MHz power coupler ; copper plating of the outer conductor (photo)

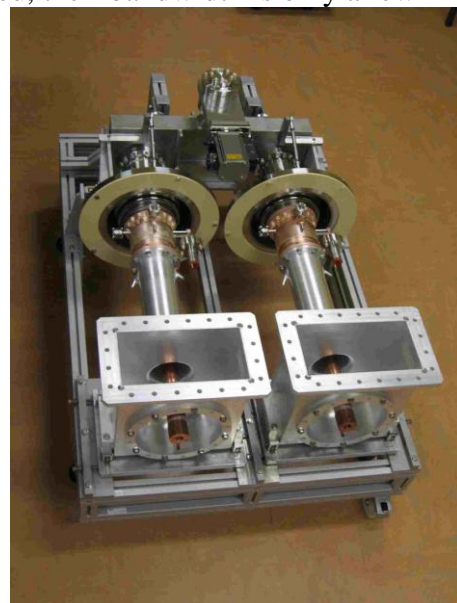


Figure 24 : Coupler test bench

The couplers are ready to be tested and conditioned on the coupler test bench (Figure 24).

In order to achieve the conditioning of the couplers and to realize further high power tests, and in agreement with the HIPPI program, a high power 704 MHz RF test place for superconducting cavities built at CEA-Saclay.

The main components of the RF test stand are a 95 kV-275kVA DC High Voltage Power Supply, a 50Hz modulator and a 1MW 704.4MHz RF klystron amplifier.

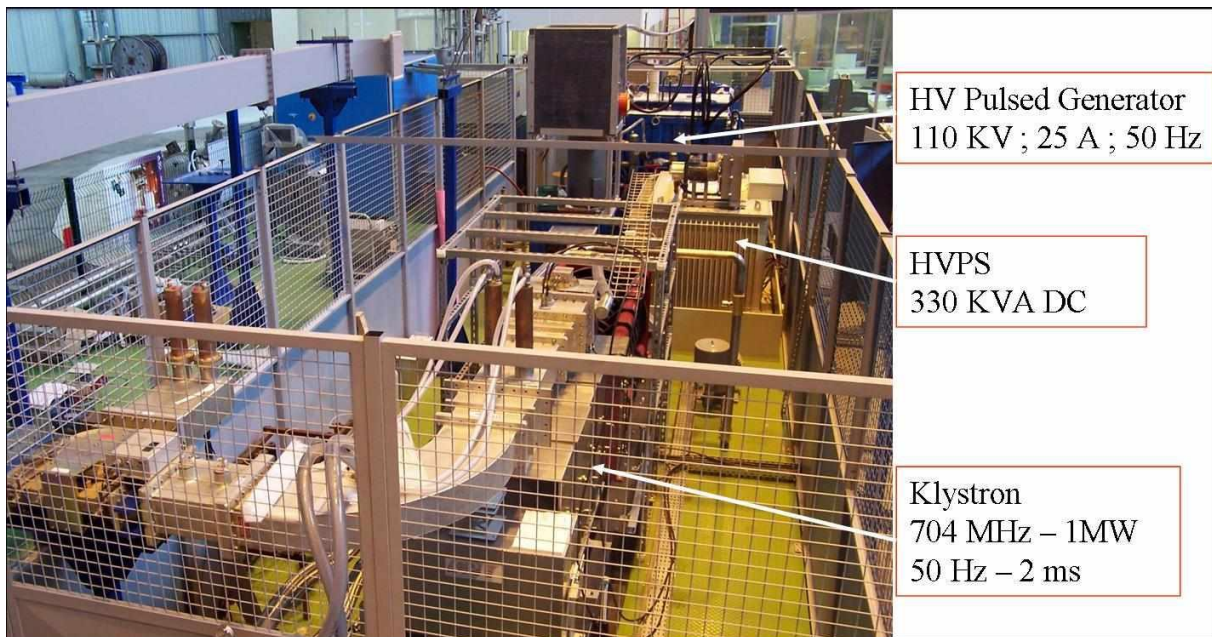


Figure 25 : 704 MHz RF test place at CEA-Saclay

IV. Cavities $\beta = 0.1$

A. General information about the prototypes – mechanicals

1. Miscellaneous

	Single Spoke IPN	CH IAF
Nominal wall thickness [mm]	3	2-3
Length of the cavity (mm) (flange to flange)	450	1050
Flanges material	St. Steel	
Helium tank material	St. Steel	N/A
Magnetic shield	Supplied by cryostat	Supplied by cryostat

Table 5 : Miscellaneous parameters

CH structure

To test superconducting cavities at the IAP in Frankfurt, a cryogenic laboratory has been established recently. The laboratory has been equipped with a 3 m long vertical cryostat, a magnetic shielding (shielding factor 30), two transport dewars for LHe, a class 100 laminar flow box and the necessary RF equipment including the control system. The cryogenic laboratory has been already put into operation. Cold tests of a 176 MHz half wave resonator built by ACCEL have started and the cavity has been operated in a phase locked loop mode.

There are different possibilities to couple RF power to a superconducting. CH-cavity. To study different coupling methods MWS simulations have been performed. On the basis of these simulations it was decided to couple electrically with a coaxial coupler through the girder. The simulations of the external Q-value could be reproduced by measurements very well.

2. Stiffening systems

Single Spoke

The 2 gaps single Spoke cavity prototype is built with 3 mm RRR 250 niobium. The cavity has been stiffened by semi-tube in front of each end cup. The helium vessel is made of stainless steel; it is connected to the cavity by stainless steel bellows.

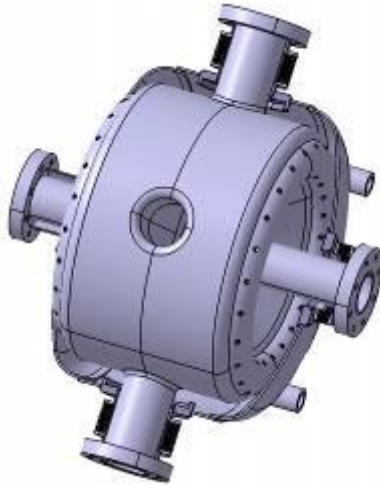


Figure 26 : stiffened single Spoke cavity with its helium vessel

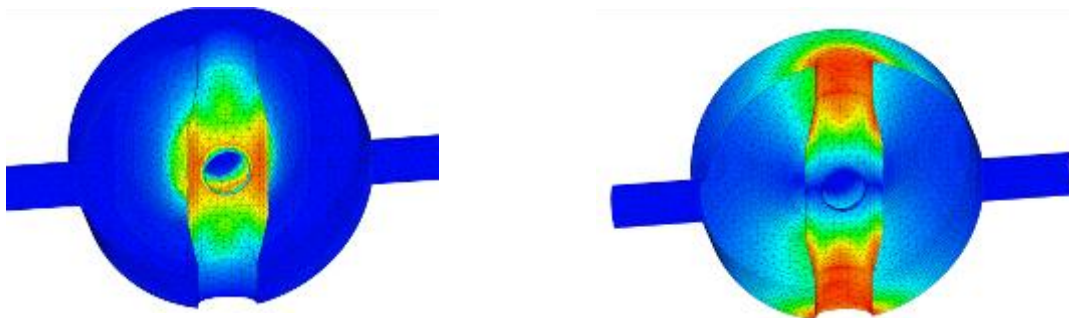


Figure 27 : Electromagnetic fields distribution on the cavity wall (left E field, right H field)

CH structure

Due to the crossed stem construction this cavity has a very high mechanical rigidity, which is needed for superconducting operation. The CH-structure has some common features with the multipole resonator. But the CH-structure uses girders to connect the stems which decrease the transverse dimensions of the cavity and results in lower magnetic peak fields. These girders are reducing the mechanical rigidity of the cavity, which necessitates some additional stiffening ribs. After a study had shown the technical feasibility of producing s.c. CH-structures the fabrication of this prototype cavity has been started in 2003 by the company ACCEL (Bergisch-Gladbach, Germany). The cavity parts are produced with 2-3 mm thick high RRR bulk niobium sheets by deep drawing and spinning. Because of the very complex geometry many procedures of the production had to be developed first. Each production step has been performed in copper including the electron beam welding.

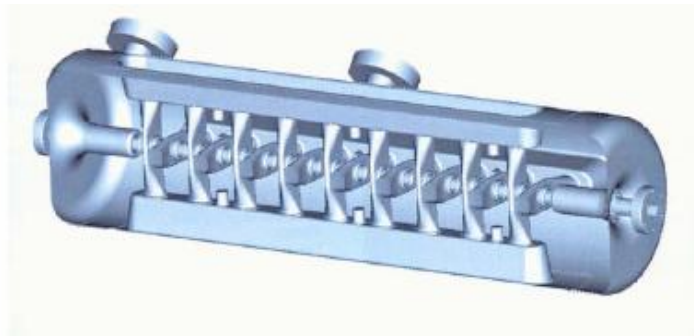


Figure 28 : MWS plot of the 19 cell CH-prototype



Figure 29 : Photo of the CH prototype before welding of the end cells

A mechanical analysis using ANSYS has been done to determine the deformation due to the external air pressure. It has been found that additional stabilization rings were necessary to stabilize the cavity. Due to these experiences it is suggested to use niobium material of 3.5 mm thickness for future applications and consequently an alternative transverse tuning concept. In a second step, the mechanical eigenmodes have been calculated. The frequencies are between 146 and 417 Hz which means that the CH-cavity is a stiff structure.

3. Mechanical parameters / comparison

	Single Spoke IPN	CH IAF - FU
Cavity stiffness K [kN/mm]	6	6.5
Tuning sensitivity $\Delta F/\Delta l$ [kHz/mm]	964	400
Pressure sensitivity [Hz/mbar] (fixed ends)	180	250
k_L with fixed ends [Hz/(MV/m) ²]	-20	-8
k_L with free ends [Hz/(MV/m) ²]	-72	
k_L measured during cold tests (detailed in next section) [Hz/(MV/m) ²]	[-55 ; -47]	

4. Tuning systems

Single Spoke

The tuning system with piezo has been developed at IPN Orsay, the tuner is inserted between flanges and helium tank of the 0.15 single Spoke cavity.

Test of tuning system with piezos

Test of the tuning system was already performed in 2007 with the stepper motor control giving a tuning range of about 300 kHz within elastic cavity deformation zone and a sensitivity of 0.94 Hz/step which is very good since we wished a resolution of 10 Hz.

In May 2008 a test with piezoelectric-actuators has been done on the tuning system. These actuators allow a fine fast tuning with a range of about 1.1 kHz which correspond to a local stroke of 11 μm made in several milliseconds. Preloading (of about 2 kN) on the piezo was done thanks to the expansion of an aluminum part by heating up.

Sensitivity of the frequency shift is about 100 Hz/ μm

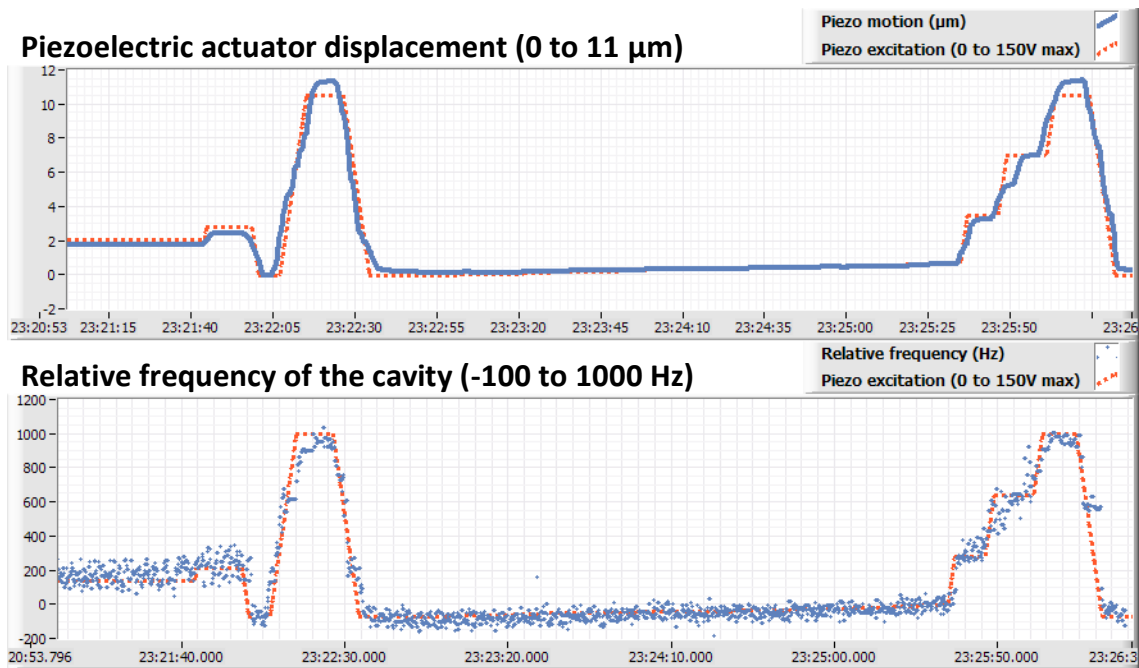


Figure 30 : Response of the cavity frequency while changing the piezoelectric length

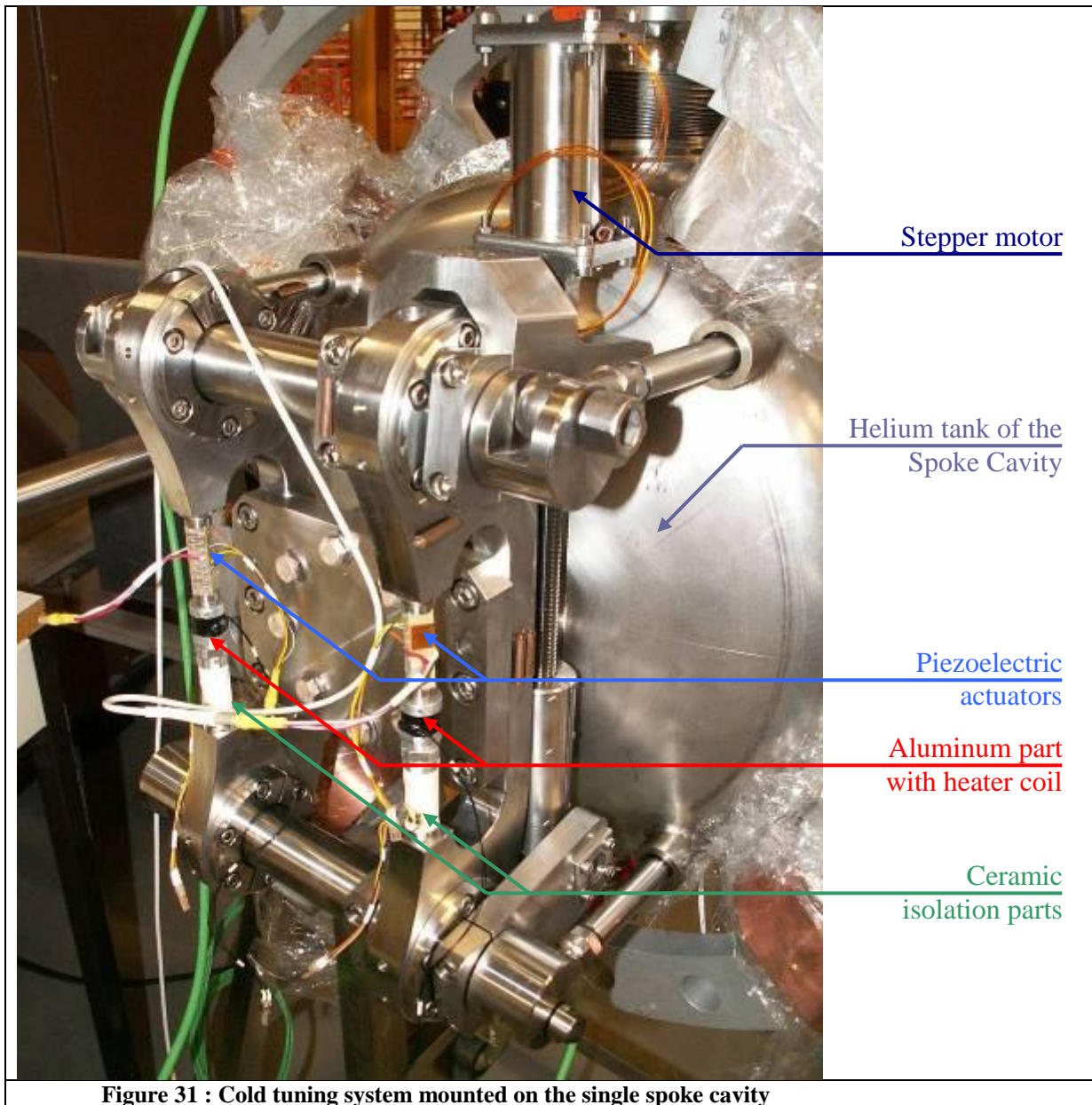


Figure 31 : Cold tuning system mounted on the single spoke cavity

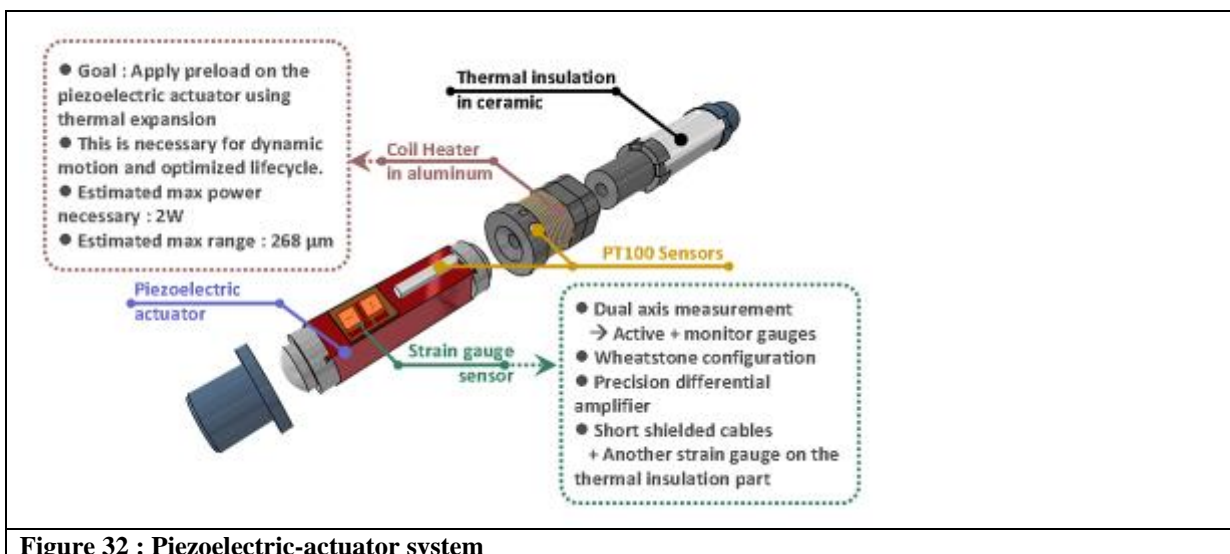


Figure 32 : Piezoelectric-actuator system

The ceramic part (in white on the picture) thermally isolated it from the rest of the tuning system. Objective of the piezoelectric-actuators system was to be able to tune the cavity with a better speed than the motor.

CH structure

The frequency tuning device comprises two stages: a slow mechanical tuner with a tuning range of $\Delta f_{\text{mech.}} = \pm 1$ MHz and a fast piezo tuner operating in an expected range of $\Delta f_{\text{piezo}} = \pm 1$ kHz. The piezos will be inserted into the beam pipe, between the inner cold mass containing the helium and the outer room temperature vacuum vessel, so that they will operate at a temperature somewhere between 4 K and 80 K, which determines their maximum stroke. The mechanical requirements of the piezos had been carefully taken into consideration during the design of the tuning system. Since they are sensitive to canting and shearing forces, their action should be very well controlled. We introduced guiding bolts and a tight over all fitting of the parts. To avoid canting the force will be transmitted to a supporting plate over a spherical surface at one end of the piezo; a rigid fixation is given only at one end.



Figure 33 : Scheme of the piezo tuner on top and one part of the tuner carrying the three piezo actuators

B. Controls and tuning of the cavity

Single Spoke

After BCP chemistry, the effective thickness of the cavity was measured, and it gave a result between 2 and 2.7 mm.

CH structure

The prototype cavity has a measured operation frequency of 360 MHz which is about 7 MHz above the design value because of the weld shrinking of the tank by 2.5 mm which was acceptable because of the broadband of the amplifier.

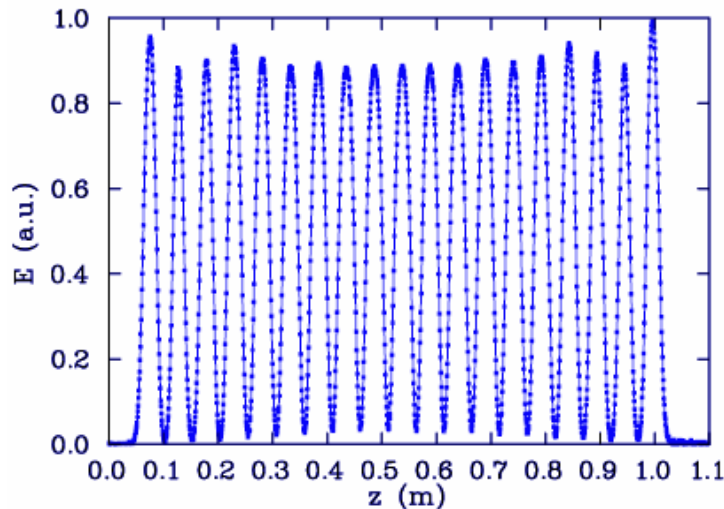


Figure 34 : Measured distribution of the electric field after the final welding.

An elastic deformation of the cavity by applying a pushing or pulling force at the end flanges of the tank changes the width of the outer most accelerating gaps and thus gives an efficient possibility to tune the rf frequency during operation. The rf-response of the cavity was simulated with MWS and by multi-physics program COMSOL. These calculations have been compared with a measurement that has been accomplished at room temperature. The force was applied by the outer corset that allows a variation of the cavity length. From simulation results a force of $F_{def.} = 6.5 \text{ kN}$ must be applied to have a deformation of $\Delta x = 1 \text{ mm}$ at both ends of the tank; $\Delta f/\Delta x = 850 \text{ kHz/mm}$ were calculated. However the measured frequency tune shift is only $\Delta f/\Delta x = 400 \text{ kHz/mm}$, which is indeed considered to be sufficient enough. The change of field distribution according to the deformation of the tank has been measured by using the bead pull method. The experimental results are in good agreement with MWS simulations. The effect is mainly concentrated on the end cells of the structure, where a maintainable maximum field variation of 10% within the tuning range was observed.

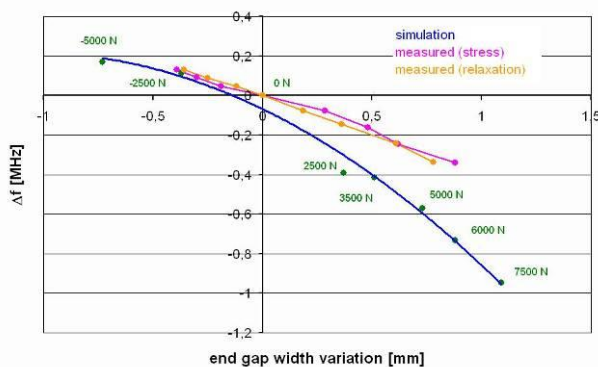


Figure 35 : Simulated and measured rf-response.

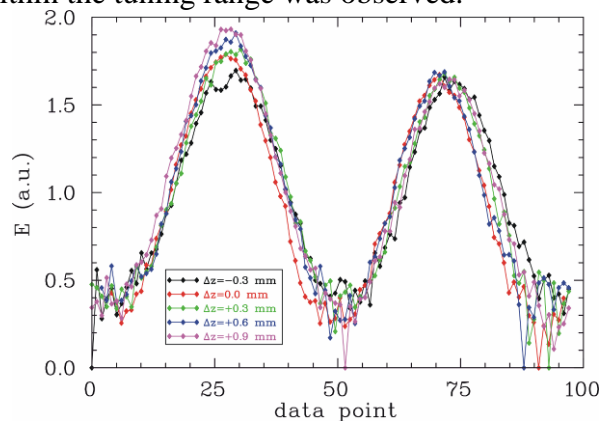


Figure 36 : Measured change of field distribution according to an end gap deformation Δx .

C. Cold tests

1. Treatments for the cavity and RF tests

Triple Spoke 760 MHz

As precised in the beginning of the report, the RF tests of a triple spoke, $\beta = 0.2$, 760 MHz cavity were also included in the HIPPI program. The results of these tests are given in this section.

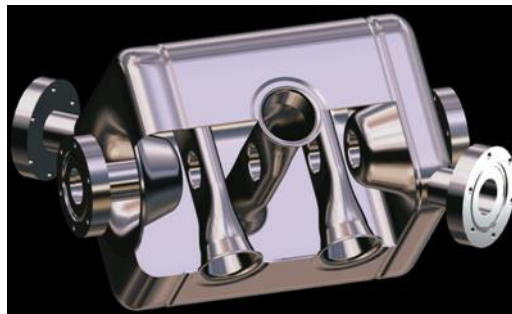


Figure 37 : Triple Spoke cavity with $\beta = 0.2$, and frequency 760 MHz

After test 1 the cavity was warmed up, disassembled, degreased and heat treated at 600°C for 10 hours. After furnace treatment, degreased and BCP with 1:1:3 in steps of 5 min each (on sample app. 0.9 microns/min); total time of BCP 30 min; then HPR in 2 locations axially with cavity rotating, app. 30 min each, R@D HPR system. Cavity dried in class 10 clean room over night and was assembled next morning (PK), then attached to test stand and evacuated, prior to cooldown, with pressure~ 1.2e-8 mbar. This was continued next day after Helium top off.

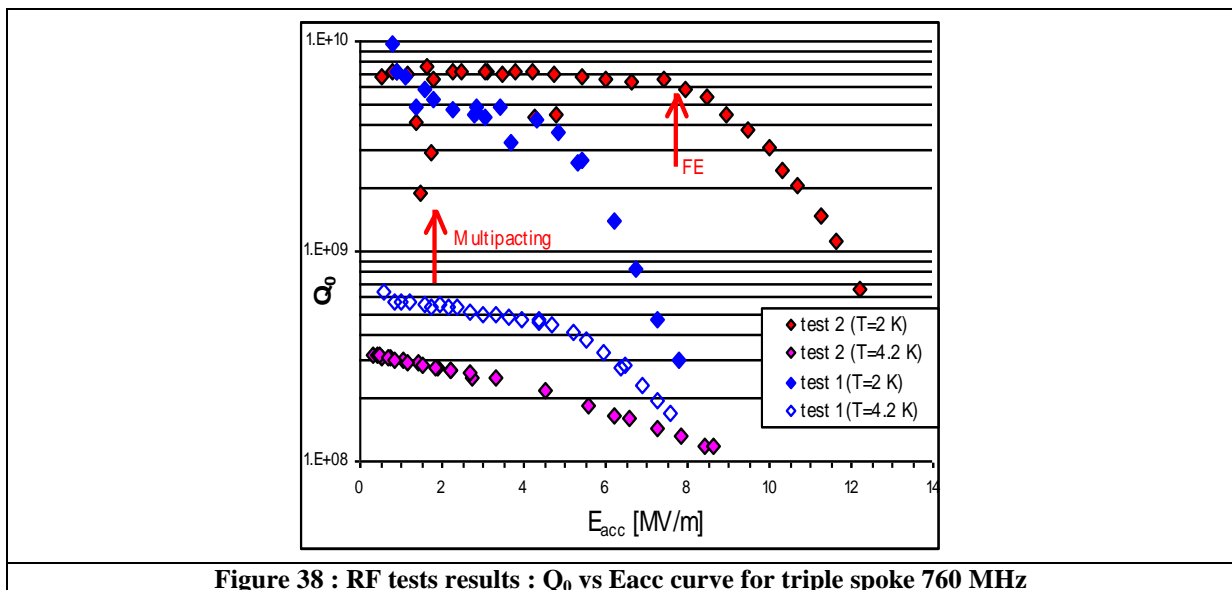


Figure 38 : RF tests results : Q_0 vs Eacc curve for triple spoke 760 MHz

Single Spoke

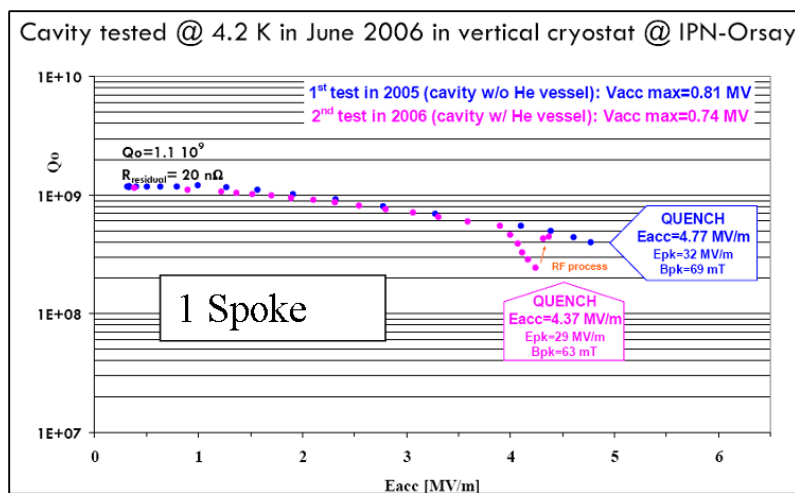
The preparation was done at CEA/Saclay, and consisted into a BCP chemistry (120 μm) and a HPR (2 hours through the 4 ports)



Figure 39 : Single Spoke chemistry at Saclay



Figure 40 : High Pressure Rinsing at Saclay

Figure 41 : RF tests results : Q_0 vs Eacc curve for triple spoke 760 MHz

CH structure

After the fabrication of the CH-prototype the structure was prepared with Buffered Chemical Polishing (BCP) and High Pressure Rinsing (HPR). Subsequent tests resulted in an effective gradient of 4.7 MV/m ($\beta\lambda$ -definition) which corresponds to electric peak fields of 25 MV/m and to an accelerating voltage of 3.7 MV, respectively. The Q-value at low field level was $5.7 \cdot 10^8$ which corresponds to a total surface resistance of 96 n Ω . The residual resistance was 43 n Ω . The limitation was field emission induced quenching. Above a peak surface field of 20 MV/m, strong field emission has been observed. The X-ray distribution has been measured with Thermo-Luminescence-Dosimeters (TLD).

After a new surface preparation performed at ACCEL including BCP and HPR gradients of 7 MV/m have been achieved. This corresponds to an effective voltage of 5.6 MV. The cavity performance has been increased by about 50% compared to the former measurements (see Figure 42); field emission activity could be reduced drastically. Especially an emission site close to the cavity centre which has been identified using Thermo-Luminescence Dosimeter (TLD) could be removed.

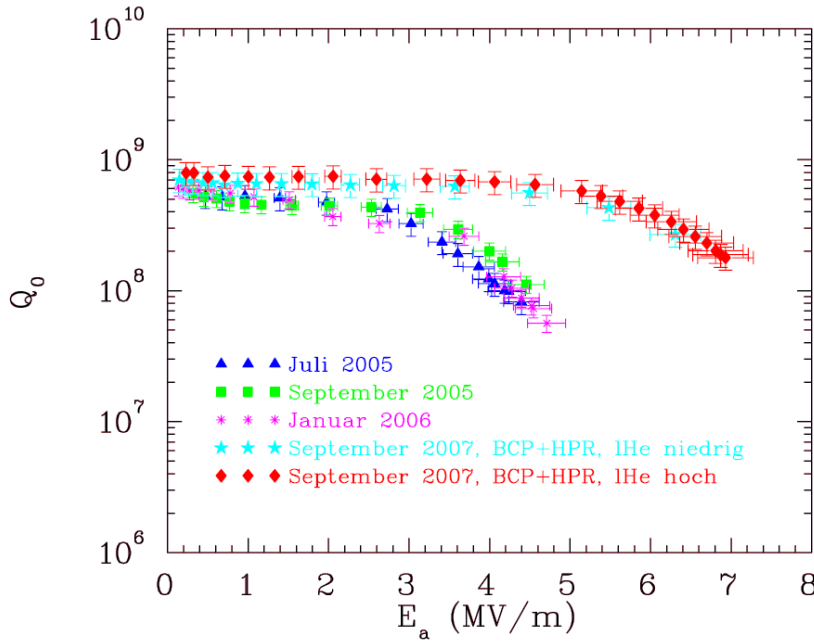


Figure 42 : Measured Q-value versus the gradient. After a new surface preparation the cavity performance has been increased significantly by reducing field emission activity.

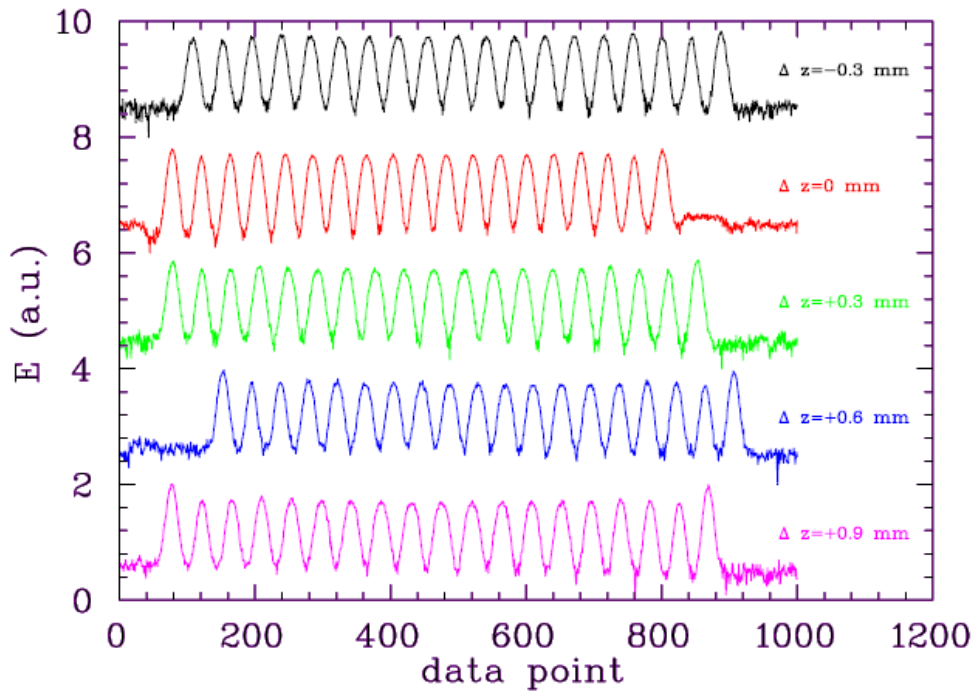


Figure 43 : Measured field distribution along the CH-cavity for different end cell deformations Δz . A field enhancement of about 10% has been observed for a Δz of 1 mm on each side. The field of the inner gaps is unaffected.

2. Mechanical measurements

Single Spoke

Several series of tests were carried out on the 2 gaps Spoke prototypes at IPN Orsay, the good agreements between simulations results and experimental data have been observed. The measured Lorentz forces factor is situated between $-55 \text{ Hz}/(\text{MV}/\text{m})^2$ and $-47 \text{ Hz}/(\text{MV}/\text{m})^2$

while the simulations predict this factor to be $-20 \text{ Hz}/(\text{MV}/\text{m})^2$ in case where the cavity is totally constrained and to be $-72 \text{ Hz}/(\text{MV}/\text{m})^2$ in case where the cavity is free. The conditions of the tests are somewhere between free ends and fixed ends considering the helium vessel's stiffness.

CH structure

Lorentz Force Detuning (LFD) was measured by observing the Voltage Controlled Oscillator (VCO) signal $U_{\text{VCO}} = 0 \dots 1 \text{ V}$ of the rf-system. This signal determines the oscillator frequency within a preset frequency range (deviation). Since the actual test system is not operating at fixed frequency, but follows the rf-variations of the cavity, the rf-detuning can directly be observed by means of the VCO signal. LFD is very precisely reproduced from pulse to pulse, but is modulated by microphonics. Mechanical resonances, which can especially be excited at pulsed operation, can reinforce the sonic effects, causing large variations of the rf-resonance. Up to a certain degree, this can be compensated by increasing the output power of the rf-amplifier, but this becomes increasingly unfeasible at higher gradients since $\Delta f_{\text{LF}} \propto E_{\text{acc}}^2$. A fast piezo tuner is an alternative to compensate the mechanical detuning.

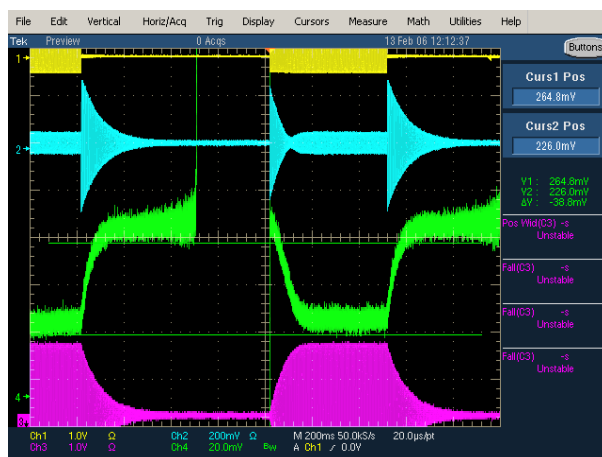


Figure 44 : The VCO signal (green) as a direct indication of LFD. Rf-pulse (yellow), Reflected power (blue), transmitted power (pink).

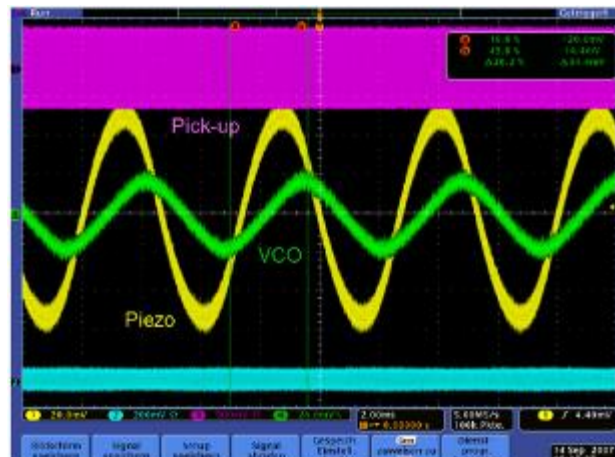


Figure 45 : One piezo drives a harmonic perturbation of the cavity. The VCO signal of the phase detector is proportional to the resonance shifting.

To avoid instabilities in the control system it is important to care about mechanical resonances of the cavity and their impact on the resonance frequency. Very low resonances can then be damped or pushed to higher frequencies if necessary. We have measured the resonances at room temperature by using one of the piezos as an actuator stimulating the cavity with either a sinusoidal signal from an acoustic wave generator or with white noise comprising all frequencies between 0 and 100 kHz, alternatively. The response of the cavity was then detected by a microphone or by a second piezo used as a detector and was digitally recorded. These wave data were Fourier analyzed subsequently.

Resonances were again observed and analyzed at cryogenic temperatures with a second piezo used as an impact microphone. In addition, the rf-detuning by the acting piezo was observed for the first time via the VCO-signal of the control system. A perfect deviation control was provided even at highest mechanical amplitudes. It is obvious that some mechanical resonances affected the VCO-signal considerably (279 Hz) while others do not (450 Hz). It is an interesting fact that especially resonances between 200 and 300 Hz can effectively be damped, which is not the case for the 450 Hz resonance; but that one can be neglected because it does not have an impact on the rf-resonance.

During these tests an active periodic cavity detuning provided by the piezo tuners was implied, while stable superconducting cavity operation was kept by a frequency control loop acting on the rf-frequency oscillator.

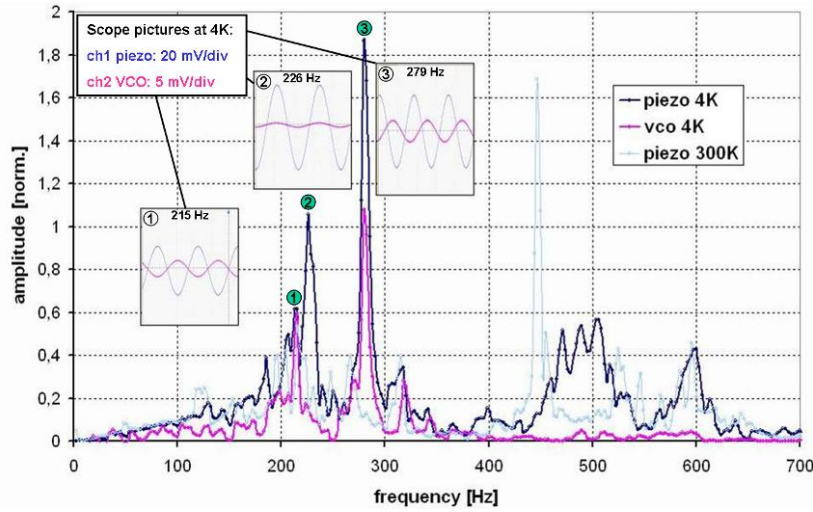


Figure 46 : Microphonics at cryogenic temperatures and the impact on the rf-resonance. Three resonances are pointed out, corresponding oscilloscope pictures are shown. Case 2 at 226 Hz can clearly be detected by the piezo sensor, but has no impact on the VCO signal.

D. RF Couplers

Single-Spoke

We have 3 models in house. These couplers have been designed for a maximum 20 kW CW operation.



Figure 47 : RF antennas for the single spoke RF coupler

Coupling cavity

A new cavity has been designed, fabricated and delivered by end of July 2008. The frequency tuning to 352 MHz has to be done (with bulk copper plungers) without problem.



Figure 48 : Old design



Figure 49 : New coupling cavity

RF coupler set on beta 0.15 Spoke cavity

Two loops (made of copper tube) have been brazed on the connecting tube between the coupler window and the cavity flange. This circuit will be cooled by liquid nitrogen and should intercept the heat flux coming from 300K.

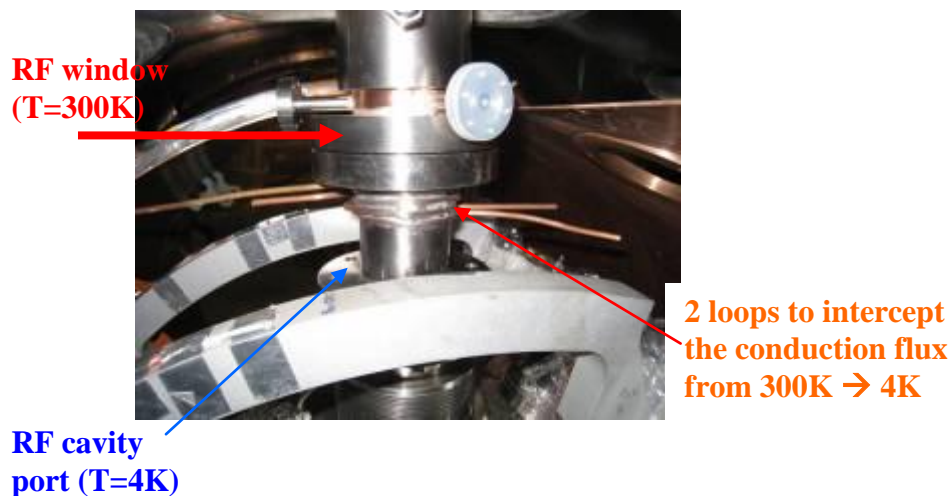


Figure 50 : RF coupler mounted on the single spoke cavity

RF test bench

The test bench is now ready. Conditioning of the couplers has started in mid-December 2008 by checking all the security processes. The ramping-up of power is foreseen in January

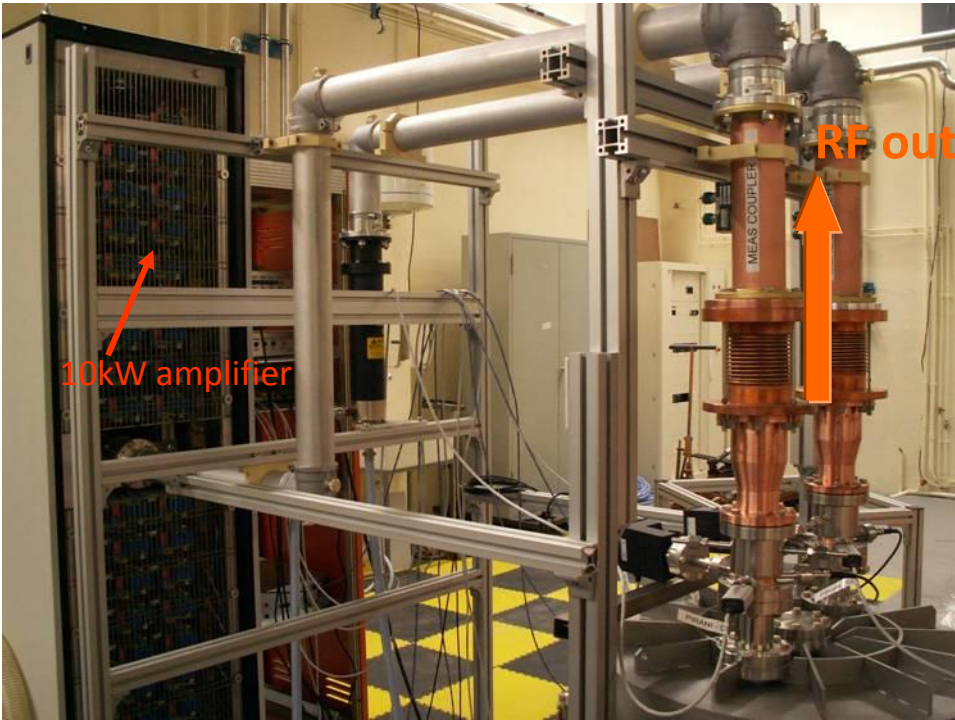


Figure 51 : RF test bench ready

V. Conclusion

The work achieved through the HIPPI-WP3 has given very significant elements about the design and fabrication of low and intermediate beta superconducting structures optimized for operation in pulsed mode. These elements, together with the measurements and tests performed on these structures, are a nice material for comparative assessment.

From the Q_0 vs E_{acc} curves presented in the previous sections, we calculate the maximum accelerating field $E_{acc} = |\Delta U|/(q.L_{acc}) = V_{acc}/(N_{gap}.\beta.\lambda/2)$ reached for each cavity type (1st line of Table 6).

Because of the differences of the structures, it is difficult to compare the results for the $\beta = 0.5$ cavities and for low β cavities. For this reason, we will only discuss about the comparison of cavities of intermediate beta. The experimental tests show that the elliptical cavities reach higher values of accelerating field than the triple spoke.

In the intermediate beta cavities, the limitation for the accelerating field is the thermal breakdown of superconductivity (quench), which occurs when the temperature is locally increased up to the critical temperature by the RF losses. Thus, a critical quantity is $R_s \cdot H_{pk}^2$, where R_s is the surface resistance of the superconducting niobium and H_{pk} is the maximum local magnetic field at the inner surface of the cavity. Thus, the expectable maximal E_{acc} should be higher for the elliptical cavities for 2 main reasons :

- B_{pk}/E_{acc} is lower for the elliptical cavities (see Table 2)
- R_s is much lower for the elliptical cavities, because they operate at 2 K, while the triple spoke operates at 4.2 K (see Table 2)

Apart from these considerations, other parameters like the shape of the cavity, the purity of the niobium and the surface cleanness have also an influence on the performances of the cavities. In particular, differences in the preparation of the cavities can lead to a large spread of Q_0 and E_{acc} values.

cavity	Elliptic A	Elliptic B	3 Spoke	1 Spoke	CH
E_{acc} max	17 MV/m	15 MV/m	5.8 MV/m	4.77 MV/m	7 MV/m
L_{acc}	500 mm	500 mm	818 mm	170 mm	810 mm
$ \Delta U $	8.5 MeV	7.5 MeV	4.7 MeV	0.81 MeV	5.7 MeV
L_{cav}	870 mm	832 mm	780 mm	450 mm	1050 mm
V_{acc}/L_{cav}	9.7 MV/m	9 MV/m	6 MV/m	1.8 MV/m	5.4 MV/m

Table 6 : Comparison of maximum accelerating field

A new value of accelerating field gradient is also calculated by using the overall length of the cavity instead of L_{acc} . This kind of real estate gradient takes into account the size of the cavity. The third line of Table 6 gives the energy received by a particle while crossing the cavity: $|\Delta U| = E_{acc} \cdot q \cdot L_{acc}$. The fourth line reminds the overall length of each cavity (see

Table 3 and Table 5), and the last line shows the results for V_{acc}/L_{cav} . The calculus of this new gradient appears to be more favourable to the elliptical cavities.

By taking into account parameters external to the cavities themselves we could define a real estate gradient more relevant for a linac structure. This should involve the intermediate space between the cavities, depending on the accelerator and cryomodule design, and cryogenic technology. This could be a further step for the comparison of accelerating structures.

VI. Acknowledgements

We acknowledge the support of the European Community-Research Infrastructure Activity under the FP6 “Structuring the European Research Area” programme (CARE, contract number RII3-CT-2003-506395)

I.	Introduction	2
A.	CARE – HIPPI / WP3	2
B.	Outline of the report	2
II.	Presentation of the cavities - RF parameters	4
A.	The cavities	4
B.	RF parameters	6
III.	Cavities $\beta = 0.5$	6
A.	General information about the prototypes – mechanicals	6
1.	Miscellaneous	6
2.	Stiffening systems	7
3.	Mechanical parameters / comparison	10
4.	Tuning systems.....	12
B.	Controls and tuning of the cavity	13
C.	Cold tests	13
1.	Treatments for the cavity and RF tests	13
2.	Mechanical measurements	16
D.	RF couplers	18
IV.	Cavities $\beta = 0.1$	20
A.	General information about the prototypes – mechanicals	20
1.	Miscellaneous	20
2.	Stiffening systems	20
3.	Mechanical parameters / comparison	22
4.	Tuning systems.....	22
B.	Controls and tuning of the cavity	25
C.	Cold tests	26
1.	Treatments for the cavity and RF tests	26
2.	Mechanical measurements	29
D.	RF Couplers.....	31
V.	Conclusion.....	34
VI.	Acknowledgements	35